Available online at www.sciencedirect.com
SCIENCE DIRECT®
Biochimica et Biophysica Acta 1604 (2003) 33–46
BIOCHIMICA ET BIOPHYSICA ACTA
BBA
www.bba-direct.com

A reduced model of the fluorescence from the cyanobacterial photosynthetic apparatus designed for the in situ detection of cyanobacteria

M. Beutler[a,b,*], K.H. Wiltshire[c], M. Arp[a], J. Kruse[d], C. Reineke[a], C. Moldaenke[e], U.-P. Hansen[b]

[a] *Max-Planck-Institut (MPI) für Limnologie, August-Thienemann-Straße 2, 24302 Plön, Germany*
[b] *Zentrum für Biochemie und Molekularbiologie (ZBM), Universität Kiel, Leibnizstr. 11, 24098 Kiel, Germany*
[c] *Biologische Anstalt Helgoland, In der Stiftung Alfred-Wegner Institut, Postfach 180, 27483 Helgoland, Germany*
[d] *Heider Strasse 5, 24106 Kiel, Germany*
[e] *bbe Moldaenke, Wildrosenweg 3, 24119 Kiel-Kronshagen, Germany*

Received 1 October 2002; received in revised form 18 February 2003; accepted 21 February 2003

Abstract

Fluorometric determination of the chlorophyll (Chl) content of cyanobacteria is impeded by the unique structure of their photosynthetic apparatus, i.e., the phycobilisomes (PBSs) in the light-harvesting antennae. The problems are caused by the variations in the ratio of the pigment PC to Chl *a* resulting from adaptation to varying environmental conditions. In order to include cyanobacteria in fluorometric analysis of algae, a simplified energy distribution model describing energy pathways in the cyanobacterial photosynthetic apparatus was conceptualized. Two sets of mathematical equations were derived from this model and tested. Fluorescence of cyanobacteria was measured with a new fluorometer at seven excitation wavelength ranges and at three detection channels (650, 685 and 720 nm) in vivo. By employing a new fit procedure, we were able to correct for variations in the cyanobacterial fluorescence excitation spectra and to account for other phytoplankton signals. The effect of energy-state transitions on the PC fluorescence emission of PBSs was documented. The additional use of the PC fluorescence signal in combination with our recently developed mathematical approach for phytoplankton analysis based on Chl fluorescence spectroscopy allows a more detailed study of cyanobacteria and other phytoplankton in vivo and in situ.

Keywords: Phycobilisome; Energy distribution model; Phycocyanin; Cyanobacteria; Fluorescence; Phytoplankton

1. Introduction

Cyanobacteria are potentially the most interesting organisms in ecological and phycological studies. Not only do they belong to the oldest organisms on the planet [1,2], but they also are extremely important primary producers [3,4]. Moreover, many of them are toxic and thus are often nuisance organisms as candidates for aquatic algal blooms [5,6]. Also, from the biophysical point of view, cyanobacteria are interesting because of their unique modes of energy transfer in the antenna.

In spite of their importance, methods of online monitoring of cyanobacteria are less comfortable and effective as compared to other phytoplanktons, where differences in fluorescence excitation and emission spectrum provide spectral signatures to characterize algal groups. The first approach by Yentsch and Yentsch [7,8] was followed by further devices [9–11] including submersible instruments [12,13]. It was the use of light-emitting diodes (LEDs) of different colors supplemented by a quantitative evaluation

Abbreviations: APC, allophycocyanin; Chl, chlorophyll; F_o, dark fluorescence; F_m, maximal fluorescence; F, steady state fluorescence; F_v, variable fluorescence; HPLC, high performance liquid chromatography; isiA, chlorophyll-binding protein; LED, light-emitting diode; PB, phycobiliprotein; PBS, phycobilisome; PC, phycocyanin; PE, phycoerythrin; PS, photosystem

* Corresponding author. Max-Planck-Institut (MPI) für Limnologie, August-Thienemann-Straße 2, Postfach 165, D-24302 Plön, Germany. Tel.: +49-4522-763324; fax: +49-4522-763310.
E-mail address: MartinBeutler@gmx.de (M. Beutler).

0005-2728/03/$ - see front matter © 2003 Elsevier Science B.V. All rights reserved.
doi:10.1016/S0005-2728(03)00022-7

by means of curve-fitting procedures that opened the access to a simple fluorescence-based method of in vivo [14] determination of different algal groups in phytoplankton including group-specific analysis of effective quantum yield at a given actinic light intensity. The application to rapid in situ depth profiling and estimation of the chlorophyll (Chl) concentrations resulted in the differentiation of three [14] or four [15,16] algal groups.

The crucial premise of evaluation by curve fitting was based on the finding that the fluorescence excitation spectra (norm spectra [15]) of the investigated groups were apparently constant. This was valid in the green, brown and mixed group (see Ref. [15] for details). However, the characteristic norm spectrum of cyanobacteria (blue group) was found to change with environmental conditions. In order to overcome this problem, the basic approach had to be extended by two features. Firstly, a model describing the energy transfer in antennae of cyanobacteria had to be developed as a basis of a new curve-fitting approach. Secondly, the information included in the fluorescence from phycobilins had to be utilized.

An adequate model has to account for the variability of the fluorescence properties in cyanobacteria resulting from variable interaction between phycobilisomes (PBSs), PS II and PS I [17–19]. In contrast to phytoplankton other than cyanobacteria, the outer light-harvesting antennae (PBSs) contain no Chl. In species containing no phycoerythrin (PE), the PBSs consist of phycobiliproteins (PB), phycocyanin (PC) and in the core regions allophycocyanin (APC). The phycobilins within the PBSs are highly fluorescent. PC emits at a maximum emission wavelength between 650 and 660 nm in vivo.

The core antennae of PS I and PS II in cyanobacteria contain Chl. The majority of Chl is associated with PS I (for details on cyanobacterial PS I, see Refs. [20–22]). However, because of the short lifetime of PS I, the contribution to overall fluorescence is small. Nevertheless, there is a significant contribution at room temperature, as becomes obvious in the measurements described here.

The reason for the variability of the cyanobacterial excitation spectra originates from adaptation mechanisms of the cyanobacterial photosynthetic apparatus to different environmental conditions [18,23–25]. Light- or nutrient-induced changes in the PC content in the PBS modify the optical absorption cross-section of the LHC and are the main cause of changes in spectral fingerprints. However, also effective Chl per PS and PS I to PS II ratio are not constant. PS II/PS I ratio depends on light intensities [26], CO_2 concentrations, nutrient supply, or on the concentration of NaCl [27,28] in the growth medium. Chl/PS can be species-dependent, or its variability can be induced by stress, e.g. iron deficiency. When cyanobacteria become limited to iron, PBSs may be degraded, and a pigment protein complex similar to CP43′ is expressed by the isiA gene (iron stress induced). Even though the operation of isiA is not fully understood, it would influence fluorometric analysis as the number of efficient Chl/PS I is increased [29–31], and nonphotochemical quenching of PS II fluorescence is enhanced [32]. Species-dependence arises also from the occurrence of Chls in monomers and trimers in PS I related to three different fluorescence emission bands at 712, 722 and 733 nm [22]. The model has also to account for the fact that Chl associated with PS II has a different fluorescence quantum yield as compared to that of PS I [33].

Further short-term variations of the energy coupling between PBS/PS I and PBS/PS II, i.e., so-called state transitions, are correlated with the redox state of the electron transport chain [19,34–36]. In state 1, PS II is supplied with more energy than in state 2. Oxidization of the plastoquinone pool and/or redox factors in the cytochrome b_6/f complex shift the system to state 1.

Most of the above problems could be overcome by the model described here and the development of a novel fluorometer employing seven excitation wavelengths and three detection channels at wavelengths of 650 nm (PC emission), 685 nm (PS II emission) and 720 nm (PS I emission), respectively [19,36]. The amounts of cyanobacterial PB and Chl can be determined with high reliability from fluorescence spectra by a model-based fit procedure [15] including one additional parameter in order to account for variations of the cyanobacterial norm spectra. Those result from the mechanisms mentioned above. Application of this model-based multispectral fluorescence analysis provided reliable results for different cyanobacterial species, under different environmental conditions also in the presence of other microalgae.

2. Materials and methods

2.1. Growth experiments

For the test of models developed in Appendix A under different environmental conditions, *Microcystis* sp. (four species), *Synechococcus* sp. (two species), *Anabaena* sp., *Aphanezonemon* sp. (three species) were grown in 0.7-l WC growth media [37] at a temperature of 18 °C for 14 days. The cultures were bubbled with air.

2.2. Growth under eight different light intensities of *Synechococcus leopoliensis*

Growth was achieved by covering culture vessels by different gray filter combinations (LEE Standard 209, 210, 211, 298, LEE filters, Great Britain) placed in front of a light tube (L 58 W/11-860, Lumilux-Daylight, Osram, Germany) resulting in 3, 6, 9, 13, 18, 25, 35 and 50 μE m^{-2} s^{-1}, respectively, as measured with the PhAR sensor Hansatech QRT 1 (Hansatech, Great Britain) in the covered glass vessels.

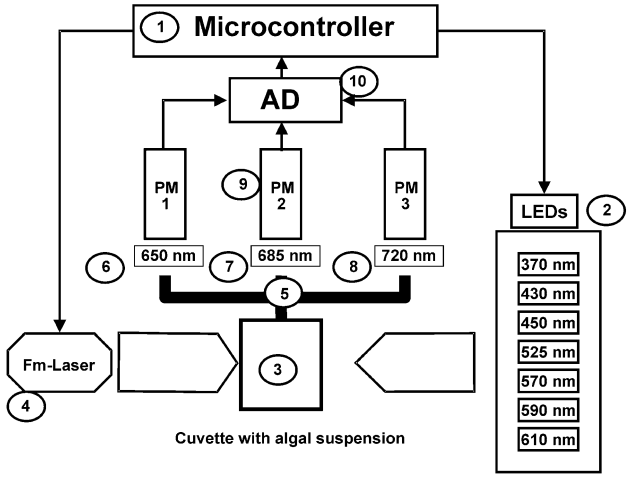

Fig. 1. Fluorometer setup: (1) microcontroller; (2) seven LEDs (measuring-light); (3) sample cuvette containing algal suspension; (4) diode laser (Fm-light); (5) multi-leg fiber bundle; (6) band-pass filter (650 nm); (7) band-pass filter (685 nm); (8) band-pass filter (720 nm); (9) three photomultipliers (PM1–3); and (10) 12-bit AD-converter (conversion rate of 500 kHz).

2.3. Growth under different sodium nitrate concentrations

S. leopoliensis was cultivated in WC medium [37]. The (sodium) nitrate concentrations were adjusted to 0.1, 0.58, 2.9, 5.9, 8.8, 12, 17.6 or 24 mmol l^{-1} by addition of different adequate concentrations of sodium nitrate.

2.4. Growth under different dipotassium hydrogen phosphate concentrations

S. leopoliensis was grown in WC medium with the phosphate component replaced by 0.0087, 0.02, 0.05, 0.1, 0.25, 0.5, 1 and 2 mmol l^{-1} K_2HPO_4.

2.5. Growth under different total nutrient concentrations

Algae were grown in mixtures of WC [37] and BG11 medium [38]. The relative amounts of BG11 medium [38] used in the eight vessels were 0%, 12.5%, 25%, 50%, 62.5%, 75%, 87.5% and 100%.

2.6. Aging cultures

To investigate the effect of the age of the batch cultures on pigment composition and fluorescence, algae were grown in a 10-l flask. After a week of initial growth, the culture was sampled on average every 3 days over a period of 30 days.

2.7. Fluorescence measurements

For the determination of norm spectra and for laboratory and in vivo experiments, a bench-top fluorometer was constructed. Fig. 1 illustrates the function of the fluorometer. Twenty-five milliliters of algal suspension could be filled in a cuvette (25 × 25 × 70 mm). Seven LEDs (370,

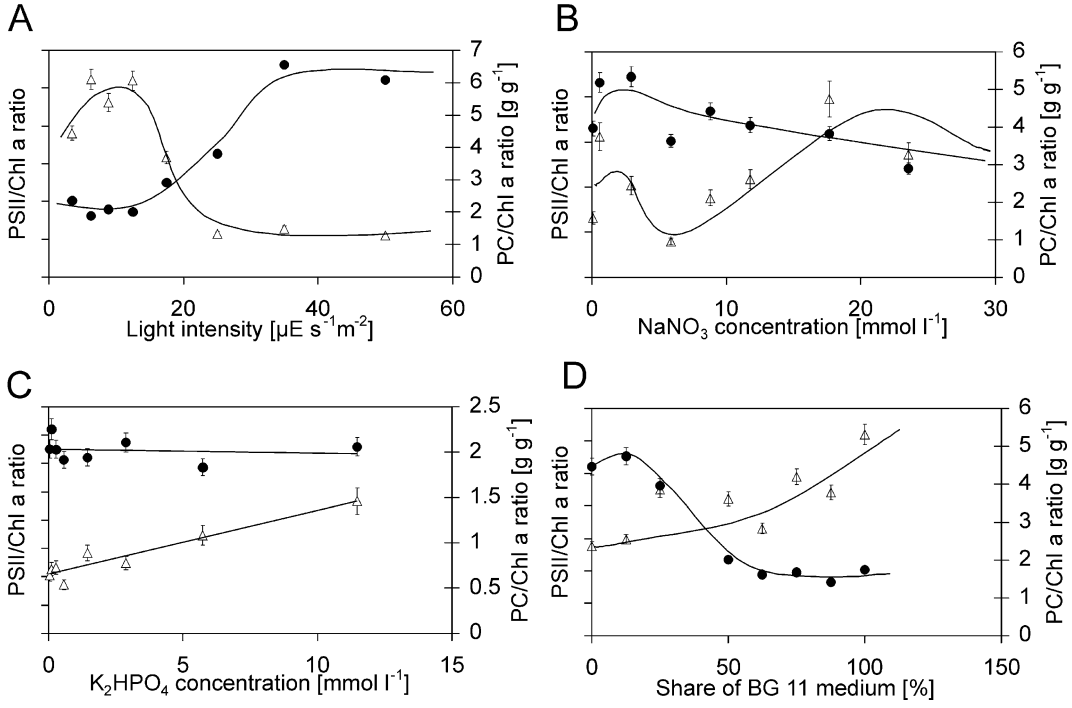

Fig. 2. Change of the pigment ratios and number of PS II reaction centers under variation of growth conditions (open triangles: ratio of PC to Chl *a*; filled circles: ratio of number of PS II centers to Chl *a* concentration). Variation of (A) growth light intensities; (B) $NaNO_3$ concentration; (C) K_2HPO_4 concentration; (D) share of BG11 medium in culture.

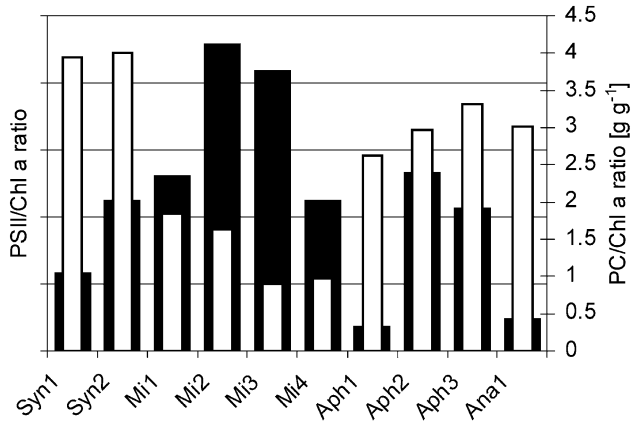

Fig. 3. Pigment ratios and number of PS II reaction centers of 10 different cyanobacterial species (open bars: ratio of PC to Chl *a*; filled bars: ratio of number PS II centers to Chl *a* concentration). Mi 1–4: *Microcystis* sp.; Syn 1,2: *Synechococcus* sp.; Ana: *Anabaena* sp.; Aph 1–3: *Aphanezonemon* sp.

430, 470, 525, 570, 590 and 610 nm) were switched on sequentially at a frequency of 5 kHz. The duration of the measuring pulse was 0.1 ms. The LED light was passed through a short-pass filter (50% transmission at 615-nm DT cyan special, Balzers, Liechtenstein) and a focusing lens. Chl fluorescence emitted by the algal suspension was coupled into the common end of a multi-leg fiber bundle (Polytec, US). The signal was detected at the end of the fiber bundle by using three photomultiplier tubes (H6779-01, Hamamatsu, Hamamatsu City, Japan) behind band pass filters (center wavelength/half width: 650/10, 685/10 and 720/25 nm. The photomultiplier signal was digitized by an AD-converter (12-bit AD-converter, conversion rate of 500 kHz) and processed by the same microcontroller (MM-103-5CAQ 18, Phytec, Mainz, Germany) used for control of the LEDs. Four laser diodes (Hitachi HL6501MG, 658 nm) with a diffuser in order to prevent sprickles were placed opposite the LEDs. These provided an additional actinic light of 3000 μmol m^{-2} s^{-1} at an area of 227 mm^2 in the cuvette. F_o, F_m, F and F_v were measured according to the definition of Van Kooten and Snel [39]. Prior to the measurement (if not otherwise stated), the algae were dark adapted for 90 s and F_o fluorescence was recorded for 60 s at an intensity of the measuring light of 0.09 μmol m^{-2} s^{-1}. Then, the laser diodes were switched on for 1 s and F_m was determined from the recorded kinetics on three detection channels for seven excitation wavelengths. This was followed by the measurement of F for 60 s at an intensity of the measuring light of 4.5 μmol m^{-2} s^{-1}.

For the experiments dealing with the influence of light intensities (state transitions), algal samples were illuminated with white light of a xenon lamp (HLX 64640, 24 V, 150 W, Xenophot, Osram, Germany) in a slide projector (3000 μmol m^{-2} s^{-1}) Gray filters (Lee Filters) were used to provide different light intensities. The samples were illuminated 15 min prior to the measurement.

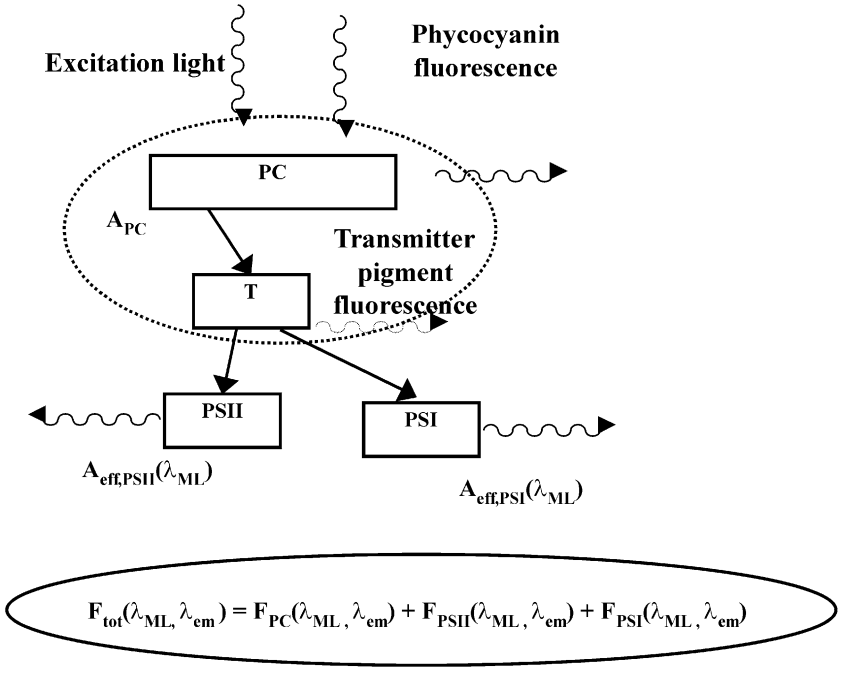

Fig. 4. Simplified model of absorption and fluorescence emission processes in PBSs and PSs in cyanobacteria (PE-free organisms like *S. leopoliensis*): $A_{eff,\ PS\ II}(\lambda_{ML})$, $A_{eff,\ PS\ I}(\lambda_{ML})$: effective absorption cross-section (in m^2) of PS II and PS I, $A_{PC}(\lambda_{ML})$: PC absorption cross-section (in m^2); $F_{PC}(\lambda_{ML}, \lambda_{em})$, $F_{PS\ II}(\lambda_{ML}, \lambda_{em})$, $F_{PS\ I}(\lambda_{ML}, \lambda_{em})$: total, PC, PS II and PS I fluorescence intensity; λ_{ML}: wavelength of measuring light; λ_{em}: fluorescence emission wavelength. The core proteins of PBS (e.g. APC) are classified as 'transmitter pigments'. The absorption and fluorescence properties of the 'transmitter pigments' were neglected in the latter consideration and reduced to the function as energy transmitters. Fluorescence model adapted and simplified from Suter and Holzwarth [61] and van Thor et al. [19].

2.8. Determination of Chl concentrations

Concentrations of Chl (for calibrating the fluorometer, see norm spectra) were determined according to Ref. [40] using high performance liquid chromatography (HPLC). The HPLC method used was a shortened version of the Ref. [41] method.

2.9. Phycobilin determination

The algal suspension was filtered through a Whatman GF/F filter. The filter was subsequently frozen at −30 °C for at least 24 h. After thawing, quartz sand and an extraction solution (0.1 M P-buffer [pH 6.8], 10 mM Na_2EDTA, LYSOZYME [0.1 mg l^{-1}] [42]) were added to the filter. The samples were then homogenized using a Teflon stick and stored in the cold at 7 °C for 12 h. Next, the samples were ultrasonicated for 130 min at 30 °C (not more than 35 °C) allowing enzyme degradation of cell walls. Then, they were centrifuged at 3600 × *g* at 15 °C for 15 min. Extracts were filtered (Spartan 30/0, 2 RC, Schleicher & Schuell, Germany, 0.2 μm pore size) and measured in a spectrophotometer (UV-DU 650, Beckman, USA). The equations for the determination of PC are given in Ref. [43].

2.10. Number of PS II reaction centers

Algal or cyanobacterial suspensions were illuminated by saturating single turnover flashes (flash duration 1 μs) from a xenon flash tube (FX 1150, EG&G, USA) with a flash frequency between 10 and 20 Hz at 20 °C. The number of evolved oxygen molecules [20] were measured in a Clark-electrode-cuvette unit (S1-electrode, DW2-cuvette-unit, Hansatech). In order to prevented potential damage of the PSs by wavelengths lower than 430 nm, an optical filter (GG435, Balzers) was inserted between the Perspex guide (length: 25 mm; diameter: 16 mm) and cuvette. Saturation of PS II by the flashes was tested with varying light intensity.

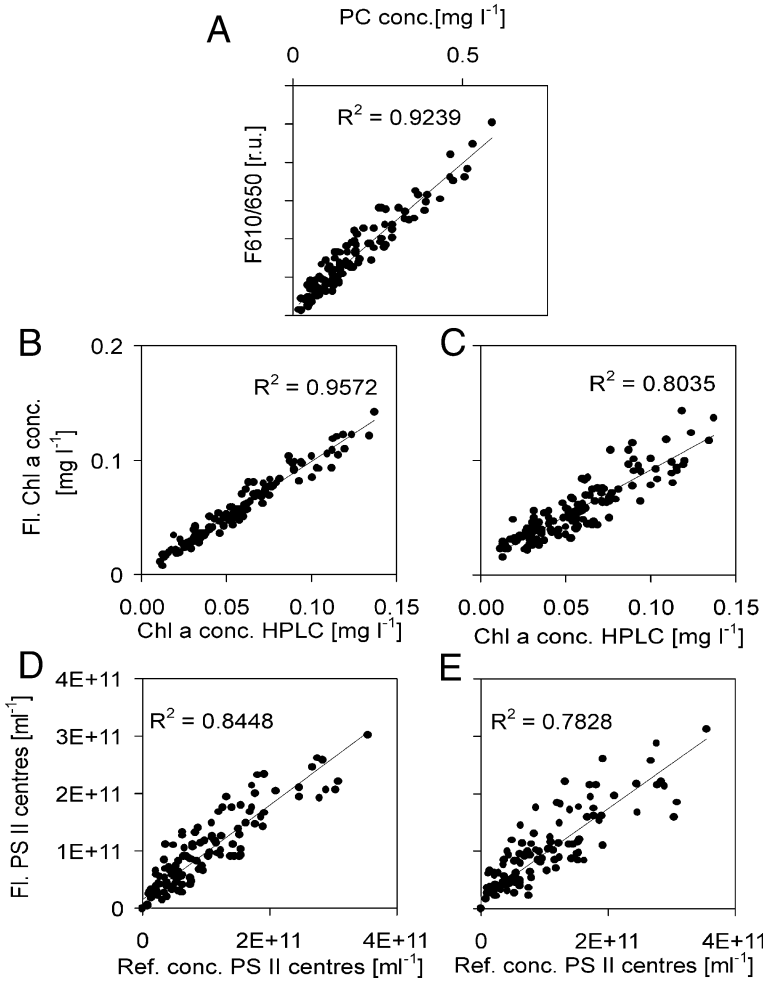

Fig. 5. (A) Dependence of the spectrophotometrically estimated PC content on the fluorescence signal $F_{610/650}$ measured at the cyanobacteria with the pigment ratios shown in Fig. 2A–D. (B–E) Linear regressions of the calculated PS II centers (estimated by oxygen flash-yield) and Chl concentrations from Eqs. (A9b) and (A16) on the reference estimates shown in Fig. 2A–D. (B) Chl *a* estimated by scenario 1; (C) Chl *a* estimated by scenario 2; (D) PS II reaction centers estimated by scenario 1; (E) PS II reaction centers estimated by scenario 2.

3. Results

3.1. Effect of pigment variability on two different evaluation problems

One task is to determine the concentrations of PC, Chl and PS II from the measured spectra in a suspension that contains no other phytoplankton besides cyanobacteria. In that case, the approach is straightforward, i.e., the variability is a result of the analysis by the model described below and does not request special precautions. The second task, however, the quantitative determination of the amounts of individual spectral phytoplankton groups in a mixed suspension (as occurring in lakes and oceans), has to cope with the problem of variable spectral properties of cyanobacteria. Here we start with the first case in order to get a survey of what effects have to be taken into account when the second problem has to be approached.

3.2. Cyanobacteria with different pigmentation for the investigation for variability of spectra and for testing the model

The influence of various growth conditions on pigment ratios in *S. leopoliensis* has been investigated by chemical methods and the results are demonstrated in Fig. 2A–D. Light intensity and total nutrient content seem to have complementary effects on PS II to Chl ratio and PC to Chl ratio, whereas the effect of P and N nutrition in Fig. 2B,C does not show such a complementary behavior. Species dependence of pigment ratios is shown for 10 different cyanobacterial species in Fig. 3. A variable ratio of PS II/Chl *a* indicates a changed ratio of PS II to PS I but could also mean an accumulation of IsiA or similar proteins that would influence this ratio by changing PS I/Chl binding [32]. The ratio of PC to Chl changed by a factor 12 in all four growth experiments (compare Fig. 2A and C) while the number of PS II centers changed five-fold. The different pigmentation types of Figs. 2 and 3 were used for the test of model developed in the next section.

3.3. A simplified model of energy transfer in the antennae of cyanobacteria

Fig. 4 shows the pigments of the photosynthetic apparatus of cyanobacteria and the flow of energy between them. The mathematical description of this model is presented in Appendix A. The application of this model to the analysis of suspensions containing only cyanobacteria is illustrated in the following sections.

3.4. Test of the first assumption with cyanobacteria of different pigmentation types (see Eq. (A8) in Appendix A)

The first assumption (Eq. (A8)) is verified by Fig. 5A showing that the same linear relationship holds between $F_{610/650}$ (fluorescence intensity measured at 610 nm excitation and 650 nm emission) and PC content for all growth

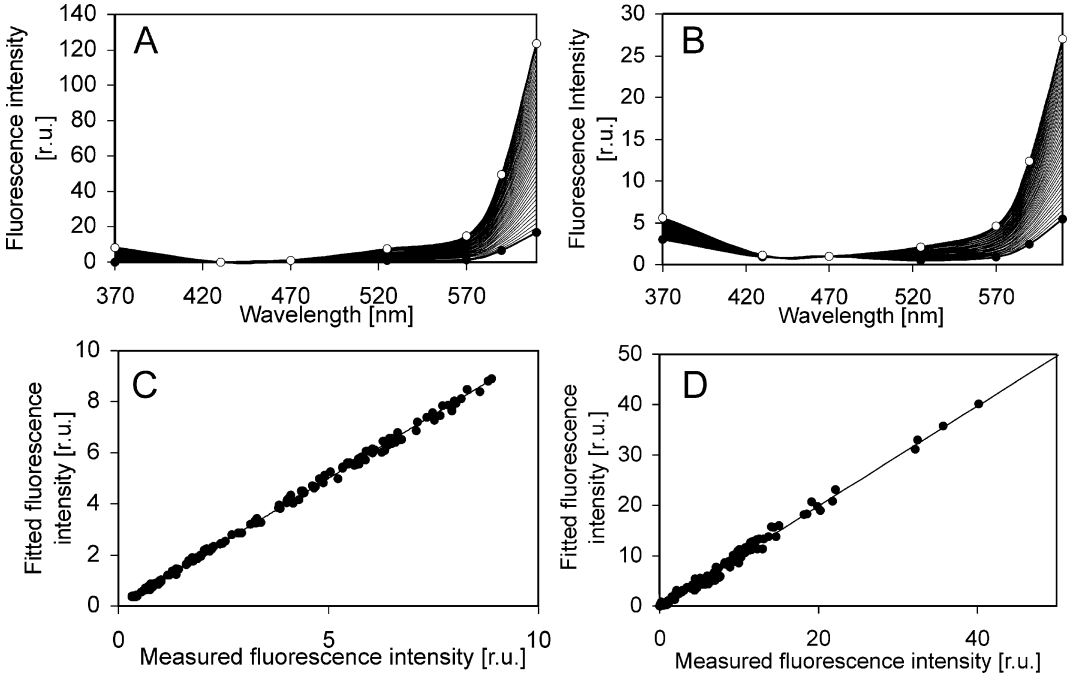

Fig. 6. Variation of cyanobacterial fluorescence excitation spectra and estimation by an artificial norm spectra matrix: (A and B) Bold lines: two extremes (defined as $\underline{\boldsymbol{c}}_{\mathrm{hi}\ \lambda\mathrm{em}}$ and $\underline{\boldsymbol{c}}_{\mathrm{low}\ \lambda\mathrm{em}}$) of fluorescence excitation spectra of the cyanobacteria with the pigment ratios given in Fig. 2. The spectra are normalized to the fluorescence intensity under excitation with 470 nm. Thin lines: artificial norm spectra matrices $\underline{\underline{C}}_{\lambda\mathrm{em}}$. (A) $\lambda_{\mathrm{em}}=650$ nm; (B) $\lambda_{\mathrm{em}}=685$ nm; (C) (650 nm); and (D) (685 nm). The correlation of measured fluorescence intensity for all excitation wavelengths at a single detection wavelength to the fitted fluorescence data by estimation of Eq. (1).

conditions employed in Fig. 2. Further, the correlation coefficient for $F_{610/650}$ to the PC content for the 10 different species in Fig. 3 was $R^2 = 0.9186$. Thus, Eq. (A8) can be used in Eqs. (A9a)–(A17).

3.5. Estimation of Chl and PS II by fluorescence in cyanobacteria

To verify the second assumption represented by Eq. (A16), the determination of total Chl *a* by means of Eq. (A9b) was compared with the results from HPLC analysis. The correct determination by fluorometric methods (Fig. 5B,C) implies that the parameters $c_{1,\mathrm{Chl}}$ to $c_{3,\mathrm{Chl}}$ of Eq. (A16) are independent of growth conditions (Fig. 2) and species (Fig. 3). Fig. 2D and E show that the coefficients of Eq. (A9b) are constant. Taking this together by means of Eq. (A17a–c) implies that also the coefficients of Eq. (A9a) are constant. Thus, the amount of Chl/PS I and of Chl/PS II is independent on growth conditions and species.

The comparison of the left-hand part and right hand-part of Fig. 5 describes the suitability of the two spectral scenarios suggested by the model in Fig. 4. In scenario 1, it is assumed that fluorescence described by the pair $\lambda_{1\mathrm{ML}} = 470$ nm and $\lambda_{1\mathrm{em}} = 685$ nm originates mainly from direct Chl excitation and thus mainly from PS I. Fluorescence related to $\lambda_{2\mathrm{ML}} = 610$ nm and $\lambda_{1\mathrm{em}} = 685$ nm is thought to be light that was absorbed by the PBS and is emitted by PS II. If fluorescence is assigned to $\lambda_{1\mathrm{ML}}$ and $\lambda_{1\mathrm{em}}$ in scenario 2, it is predominately light emitted from PS I (720 nm) excited by 610 nm, which was originally absorbed by the PB. The second wavelength is the same as in scenario 1.

We therefore define:

$$\text{scenario 1}: \quad \lambda_{1\mathrm{ML}} = 470\ \mathrm{nm},\ \lambda_{1\mathrm{em}} = 685\ \mathrm{nm}$$

$$\lambda_{2\mathrm{ML}} = 610\ \mathrm{nm},\ \lambda_{1\mathrm{em}} = 685\ \mathrm{nm}$$

and

$$\text{scenario 2}: \quad \lambda_{1\mathrm{ML}} = 610\ \mathrm{nm},\ \lambda_{1\mathrm{em}} = 720\ \mathrm{nm}$$

$$\lambda_{2\mathrm{ML}} = 610\ \mathrm{nm},\ \lambda_{2\mathrm{em}} = 685\ \mathrm{nm}$$

The results shown in Fig. 5B–E demonstrate a better correlation for scenario 1 for the estimation of both the Chl and the PS II center concentrations for the growth conditions in Fig. 2. Additionally, we tested scenarios 1 and 2 for different cyanobacterial species with pigment ratios shown in Fig. 3. The correlation coefficients were in scenario 1: $R^2 = 0.9772$ for Chl and $R^2 = 0.9429$ for PS II center concentration; and in scenario 2: $R^2 = 0.6959$ for Chl and $R^2 = 0.649$ for PS II center concentration. Thus, scenario 1 was found to be superior to scenario 2 in determination of PS II centers and Chl concentrations. Because of these results, the following considerations are based on scenario 1.

3.6. Variation of cyanobacterial fluorescence excitation spectra

The analysis holds only for suspensions containing no other phytoplankton besides cyanobacteria. Thus, evaluation was quite simple. However, in the presence of other phytoplankton, curve fitting has to be employed to separate algal groups [15]. In order to incorporate the variable spectra of cyanobacteria, a parametric description of this variability is necessary. Fig. 6 shows the norm spectra used for the evaluation of cyanobacteria spectra for the 650 and 685 nm channels. They are positioned between two measured extreme excitation spectra of fluorescence (defined as vectors $\underline{\boldsymbol{c}_{\mathrm{hi}\ \lambda\mathrm{em}}}$ and $\underline{\boldsymbol{c}_{\mathrm{low}\ \lambda\mathrm{em}}}$ shown as bold lines with circles). They were selected from the spectra of the pigmentation types (shown in Figs. 2 and 3 as bold lines with circles). The spectra were normalized to the fluorescence intensity excited by 470 nm.

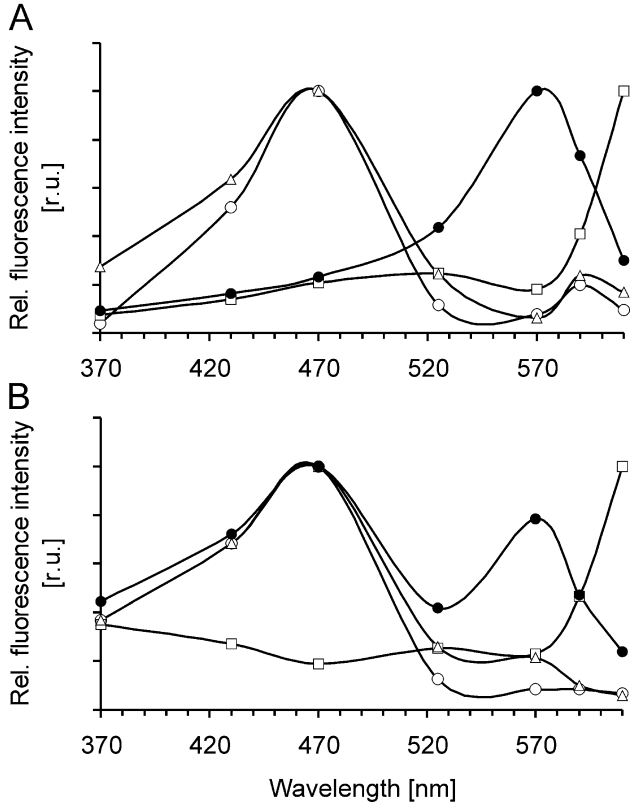

Fig. 7. Fluorescence excitation spectra of four spectral algal groups obtained with the fluorometer setup of Fig. 1 normalized to maximum. (A) Spectrum at 650-nm detection wavelength. (B) Spectrum at 685-nm detection wavelength. Green spectral group (open circles): *Chlorella vulgaris*; blue spectral group (open squares): *S. leopoliensis*; brown spectral group (open triangles): *Cyclotella* sp.; mixed spectral group (closed circles): *Cryptomonas* sp. The spectra differ significantly and can be used as norm spectra in spectral analysis.

Forty lines between these two extreme curves were calculated by linear interpolation as follows

$$\underline{\boldsymbol{c}_{l_{\lambda em}}} = (l_{\lambda em}/40)\underline{\boldsymbol{c}_{\mathrm{low}\lambda em}} + (40 - l_{\lambda em})/40\underline{\boldsymbol{c}_{\mathrm{hi}\lambda em}}$$

$$\text{for } l_{\lambda em} = 1 \text{ to } 40 \qquad (1)$$

with $l_{\lambda em}$ = number of spectra between the extreme curves in Fig. 6. The assumptions of Eq. (1) were verified by the test described below.

In order to find out whether there is one adequate $\underline{\boldsymbol{c}_{l_{\lambda em}}}$ (Eq. (1)) in the whole ensemble that describes the excitation spectra of natural samples with sufficient precision (i.e. deviation less than 5%), all $\underline{\boldsymbol{c}_{l_{\lambda em}}}$ were fitted to the measured spectra of the cyanobacteria in Figs. 2 and 3 by the following procedure. For each of the 40 $\underline{\boldsymbol{c}_{l_{\lambda em}}}$ ($1 < l < 40$), the deviation of the measured spectrum $\boldsymbol{c}_{\mathrm{m},\lambda ex,\lambda em}$ and adequate multiple of $\boldsymbol{c}_{\mathrm{l},\lambda ex,\lambda em}$ was described by the error

$$e^2_{\mathrm{lex,l}} = \sum_{\lambda ex}(\boldsymbol{c}_{\mathrm{m},\lambda ex,\lambda em} - s_{\mathrm{l}}\boldsymbol{c}_{\mathrm{l},\lambda ex,\lambda em})^2 \qquad (2)$$

with s_{l} accounting for the actual concentration.

This resulted in a minimum value of $e^2_{\mathrm{lex,l}}$ for one l (the number of the norm vector describing this particular spectrum of cyanobacteria). This is illustrated in Fig. 6C,D. The fitted fluorescence is obtained from the components of the vector s_{l} $\underline{\boldsymbol{c}_{l_{\lambda em}}}$. Thus, each $\underline{\boldsymbol{c}_{l_{\lambda em}}}$ results in seven points for the seven wavelengths in Fig. 6A,B. The measured fluorescence delivers the components of the vector of the measured spectrum. The different wavelengths are not indicated as only the location on the $x = y$ line is of interest. The average deviation from the fitted to the measured data was lower than 3%. A number of $l_{\lambda em}$ higher than 40 did not increase the precision.

For fitting measured spectra of unknown samples, a matrix $\underline{\underline{C_{\lambda em}}}$ of artificial cyanobacterial norm spectra was used ($\underline{\underline{C_{\lambda em}}}$). The rows $\underline{\boldsymbol{c}_{l\lambda em}}$ of $\underline{\underline{C_{\lambda em}}}$ are the thin lines in Fig. 6A,B as calculated by Eq. (1). By using a discrete matrix $\underline{\underline{C_{\lambda em}}}$ for the cyanobacterial norm spectra, we saved calculation time in a fit procedure for the estimation of algal groups (described in Appendix B).

3.7. Norm spectra of other spectral algal groups

To determine pigments of cyanobacteria in a mixture of different algal species, it is necessary to account for the presence of other phytoplankton. This can be achieved by including norm spectra for other phytoplankton in a mathematical fit. Norm spectra were recorded on the 650

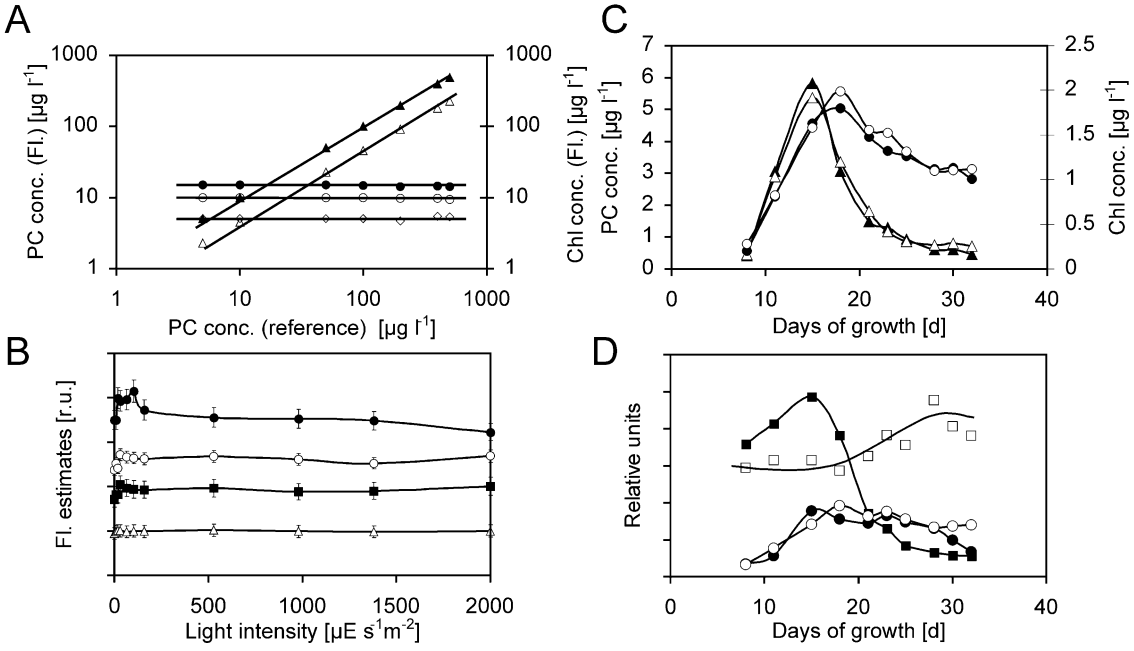

Fig. 8. (A) Variation of contribution of blue algal group in the presence of other phytoplanktons. The fluorometrical estimate of the Chl (green: closed circles; blue: open triangles; brown: open diamonds; mixed: open circles) content and the fluorometrically determined PC content (closed triangles) is shown versus the spectrochemically determined PC content of the blue group. (B) Fluorometric pigment and PS II reaction center estimates under light adaptation with different light intensities—closed circles: energetic coupling of PBSs to PS II in terms of the ratio $F_{\mathrm{v}\ 610/685}$ to $F_{\mathrm{v}\ 470/685}$; open triangles: flurometrically determined PC concentration; open circles: fluorometrically determined Chl concentration; closed squares: fluorometrically determined PS II reaction centers. (C and D) Pigment concentrations measured at different ages (in days) of a cyanobacterial batch culture. (C) PC and Chl concentrations—open triangles: fluorometrically determined PC concentration; closed triangles: reference PC concentration; open circles: fluorometrically determined Chl concentration; closed circles: reference Chl concentration. (D) Open circles: fluorometrically determined PS II reaction centers; closed circles: reference PS II reaction centers; closed squares: reference ratio PC to APC amount; open squares: energetic coupling of PBSs to PS II in terms of the ratio $F_{\mathrm{v}\ 610/685}$ to $F_{\mathrm{v}\ 470/685}$.

and 685 nm detection channel. The spectra are shown in Fig. 7 for four different species. These norm spectra were used as elements of matrix $\underline{\underline{N_{\lambda em,l_{\lambda em}}}}$ in the fit described in Appendix B.

3.8. Tests under several conditions

In a first run, the fit routine of Appendix B was tested in a dilution experiment with just one cyanobacterial group (*S. leopoliensis*). This showed that the correct $\underline{\boldsymbol{c}_{l_{\lambda em}}}$ was automatically selected, and correspondence between fluorescence analysis and amount of cyanobacterial PC, Chl, PS II centers was verified. PC concentrations as low as 1 μg l^{-1} were determined with an average error below 5% (data not shown).

A more complex test, i.e., determining the contribution of the blue algal group (*S. leopoliensis*) in the presence of other phytoplankton is shown in Fig. 8A.

Fig. 8B–D show the performance of the new approach under different conditions. The influence of changed light intensity on the fluorometric pigment and PS II center concentration estimates (Fig. 8B) was investigated. The ratio of $F_{v610/685}/F_{v470/685}$ ($F_v = F_m - F_0$) is a relative measure of energy reaching PS II by light absorption and transfer from the PBS to PS II ($F_{v610/685}$) and energy reaching PS II by light absorption of PS II directly ($F_{v470/685}$). $F_{v610/685}/F_{v470/685}$ was highest when the samples were adapted with light intensity in the range of the growth light (between 10 and 100 μE m^{-2} s^{-1}). This is similar to results of Campbell and Öquist [44]). The light-induced change of the pigments was below 10%.

In Fig. 8C,D, the pigment concentrations and energetic coupling to PS II during an aging experiment of a batch culture are shown. The fluorometrically determined values of PC, Chl and PS II center (closed circles and triangles) were in good agreement with the reference data (open circles and triangles). The energetic coupling of PBSs to PS II centers (Fig. 8C, closed squares) increased at low PC to APC ratio (open squares). This was probably due to the fact that a higher contribution of light was absorbed by APC than by PC, and energetic coupling of APC to PS II is of course higher than that of PC via APC to PS II. The energetic coupling (Fig. 8D) decreased between days 30 and 32, presumably as result of degradation processes within the core region of the PBSs. The fluorometrical determination of PS II leads to a higher result than the reference method on days 30 to 32.

4. Discussion

4.1. Applicability of the model in Fig. 4 for the estimation of cyanobacterial pigments

The comparison of chemically determined amounts of PC, Chl and PS II with the values obtained from fluorescence (Figs. 2, 3 and 5) verifies that the model in Fig. 4 is a suitable basis of the fluorometric analysis of cyanobacteria. This also implies that the assumption 1 (PC can be evaluated from the $F_{610/650}$ signal) and the assumption 2 (amount of Chl per PS II and PS I is constant) hold under the investigated conditions. The variability of the cyanobacterial antennae (as provided by the conditions in Figs. 2 and 3) does not corrupt the fluorometric analysis when this variability is restricted to the number of pigments. It has to be analyzed whether the reliability of fluorometric determination suffers if fluorometric properties and coupling ratios are changed.

Thus, the reliability of the analysis depends on whether the gross rate constants $k_{1,\lambda ML,\lambda em}$ to $k_{5,\lambda ML,\lambda em}$ from Eqs. (A7a)–(A7e) in Appendix A are constant, or, if they are not constant, have only minor influence on the coefficients in Eqs. (A9a), (A9b) and (A16). The only source of variability in $k_{1,\lambda ML,\lambda em}$ to $k_{5,\lambda ML,\lambda em}$ is in the fluorescence yields $\Phi_{F,PC}$, $\Phi_{F,PS\ II}$ and $\Phi_{F,PS\ I}$ and in the energy transfer yields $\Phi_{T,PS\ I}$ and $\Phi_{T,PS\ II}$. Several workers [19,36,45–47] have shown that the fluorescence quantum yields $\Phi_{F,PC}$, $\Phi_{F,PS\ II}$, $\Phi_{F,PS\ I}$ are approximately constant under the experimental conditions employed here, i.e. when the cyanobacteria are given enough time to adapt to the prevailing light intensities.

Experiments have not been done under conditions of iron-deficiency as the impact to develop the approach described here came from limnological projects [15]. Especially in oceans, iron deficiency may cause a strong reduction of PBS and the expression of the isiA gene leads to increased deactivation in PS II (decreasing O_2 evolution and fluorescence yield, i.e., $\Phi_{F,PS\ II}$ [48,49]) and to an increase of the effective antenna size of PS I by 60% [32] to 100% [50], thus changing $\Phi_{F,PS\ I}$. The change in the number of PBS can be handled by our approach as PBS determination requires only Eq. (A8). In the case of PS I, at least Chl content associated to PS I may be estimated correctly. However, whether the underestimation of PS II is caused by isiA-induced high fluorescence quenching [32,50] remains to be investigated.

In the two scenarios defined in Results, $F_{610/685}$ is used. The main part of this fluorescence emission originates from light energy absorbed by PC, transferred to PS II ($\Phi_{T,PS\ II}$) and emitted as fluorescence. The range of the reported values of $\Phi_{T,PS\ II}$ is between 1 and 0.9 [19,36]. This maximum change of about 10% causes an even smaller change in the calibration coefficients $c_{2,PS\ I}$ and $c_{2,PS\ II}$ (Eqs. (A9a) and (A9b)) as the related $k_{4,\lambda ML,\lambda em}$ (Eq. (A7d)) is part of a sum including other gross rate-constants. If an increase in $\Phi_{T,PS\ II}$ occurs concomitantly with a decrease in $\Phi_{T,PS\ I}$ (state transitions [19,36]), then the effect is even smaller (Eqs. (A10) and (A13)). In contrast, the reported range of $\Phi_{T,PS\ I}$ 0 to 0.1 [19,36] seems to imply major changes. Fortunately, $\Phi_{T,PS\ I}$ does not play a major role in scenario 1 ($F_{470/685}$ and $F_{610/685}$), and thus its variability can be ignored.

Scenario 2 makes use of $F_{610/720}$ that is strongly influenced by light energy absorbed by PC and transferred to PS I. Fig. 5E shows that the resulting influence on $k_{4,\lambda ML,\lambda em}$ (Eq. (A7d)) corrupts the calibration factor $c_{2,PS\ I}$ in Eq. (A9a) via Eq. (A10). Thus, PS I determination should be based on the $F_{470/685}$ signal of scenario 1.

However, it has to be mentioned that scenario 1 (using $F_{470/685}$ and $F_{610/685}$) yields more reliable results regarding PS II centers and total Chl concentration as compared to scenario 2 ($F_{610/720}$ and $F_{610/685}$).

Regardless of the above caveats, application to a wide range of species under different conditions (Figs. 2 and 3) has shown that the model-based evaluation of cyanobacterial pigments is quite reliable.

4.2. Variation of cyanobacterial pigments

For the separation of cyanobacterial pigment amount from that of other phytoplankton, the above biophysical problems of antenna organization play a minor role because Fig. 8 shows that the concept of parameter-dependent norm spectra (Appendix B) can handle all variations that have occurred in our investigations. Selecting 40 norm curves out of the two-dimensional field of the weighted sum of the two extreme curves $\underline{\boldsymbol{c}_{hi\ \lambda em}}$ and $\underline{\boldsymbol{c}_{low\ \lambda em}}$ (Fig. 6A,B) reduces the parameters from two to one providing the benefit that the fit-procedure has only one nonlinear parameter l (Eq. (B1)). Fig. 6C,D demonstrates the success of this strategy for the different excitation spectra shown in Fig. 2.

The most important feature is that all 40 norm spectra $c_{l,\lambda em}$ (Fig. 6) are linear-independent from the norm spectra of the other phytoplankton. This has the important consequence that an error in the determination of one group of phytoplankton cannot be compensated by errors in the other groups. The reliability is verified by the dilution experiments of Fig. 8A where the cyanobacterial norm spectra and the pigment concentrations of diverse algal groups were correctly estimated. This parametric description (Eq. (1)) is the key for overcoming the fit problems originating from the great variability of the fluorescence excitation spectra.

The application of the nonlinear fit procedure to selected samples deals with some important situations. Fig. 8C,D demonstrates the correct assessment of pigments during aging of a batch culture. This is a situation that might occur during a natural phytoplankton bloom. It demonstrates that scenario 1 and the fit procedure also hold for degrading pigment systems. Changing light illumination over a time scale of minutes can induce photoinhibition and energy state transitions (PBS coupling). We found that the highest deviation for pigment estimation caused by state transitions and photoinhibition together was less than 10% (Fig. 8B). The small variation of $F_{610/650}$ is not surprising as the fluorescence emission originates from PC and not from regions of the PBS where the change in energy transfer and photoinhibition takes place.

The employment of only two detection wavelengths (650 nm, Eqs. (A7a)–(A7e); and 685 nm, scenario 1) as implied by the usage of scenario 1 enables the construction of a simpler instrument. The usage of only three adequate signals out of 28 in scenario 1 or 2 is important for online analysis as it saves computer time.

The evaluation of the contribution of individual pigments by the algorithms of Appendix A can also solve the problem of the estimation of true photochemical yield in cyanobacteria [19] that is corrupted by the interference with the PC fluorescence emission in approaches not based on curve-fitting. The estimation of photochemical yield does not even suffer from inconstant parameters $k_{1,\lambda ML,\lambda em}$ to $k_{5,\lambda ML,\lambda em}$ from Eqs. (A7a)–(A7e) in Appendix A discussed above because the relationship between fluxes and relative changes in fluorescence is not influenced by changes in $\Phi_{F,PC}$, $\Phi_{F,PS\ II}$, $\Phi_{F,PS\ I}$, $\Phi_{T,PS\ I}$ or $\Phi_{T,PS\ II}$.

The principle of parameter-dependent norm spectra can be transferred to other algal groups like red cyanobacteria ($\lambda_{em}=570-580$ nm [51]) or cryptophytes. This can be achieved by an extension of the set-up in Fig. 1 with further detection wavelengths between 590 and 630 nm for the measurement of other phycobilin emissions such as PE of red cyanobacteria ($\lambda_{em}=570-580$ nm [51]) or cryptophytes ($\lambda_{em}=590-620$ nm [51]). Such an extension would solve adaptation problems that might occur in red cyanobacteria and would enable the differentiation between cryptophytes and red cyanobacteria.

Acknowledgements

We are grateful to Rolf Lippold for help with the set-up of the fluorometer. We thank Holger Dau (FU-Berlin) and Winfried Lampert (MPI, Plön) for scientific advice and support. This work was funded by the German BMBF (project number 03F0287A).

Appendix A. Energy distribution model

The model in Fig. 4 is based on investigations of energy transfer in the cyanobacterial photosynthetic apparatus dealing with energy flux in PBSs in the antenna of cyanobacteria [52,53]. They were carried out by fluorescence and absorption studies in the pico- or nanosecond range [54–60].

In PBSs of *S. leopoliensis* 6301 with no PE at photon densities of 10^{11} photons/cm^2 below energy is distributed within the PC rods with time constants of ~ 20 ps [61,62]. In trimers or hexamers of PC or APC, the equilibrium of excitation energy is extremely fast by weak excitonic interactions [62] as in PC monomers exciton transfer becomes important at donor acceptor distances below 2 nm [63–65]. APC is included in the PBS unit, as the main energy transfer process from PC to APC is Förster-transfer with rates of ~ 45 and ~ 120 ps.

Transport of energy from PBSs to PS II or PS I [26,66–69] competes with loss processes (fluorescence and non-radiative decays). Energy transfer from PC via APC and core proteins to PS II or PS I is downhill in static measurements (microsecond range and higher [19,65]). Thus, the assumption of REE (rapid excitation equilibrium) in cyanobacteria does not involve all antenna pigments as it does in chlorophyta. This implies that PS I and PS II have to be considered as separate kinetic units.

For PBS-containing organisms, the excited state equilibration within the PS II core antenna is still under scrutiny, but it is highly likely that the assumption of REE for the PS II core antenna is sufficiently good. The energy transfer through the core pigments is very efficient and is thought to exceed 95% [17]. The assignment of the antenna pigments to three REE units (Fig. 4) leads to the following mathematical description.

A.1. Fluorescence of PC in PBS-containing algae

The following equations are only valid for algal suspensions that are sufficiently optically thin. Additional terms that correct for mutual shading of algae and for fluorescence reabsorption would otherwise be required. Thus, the fluorescence intensity of the pigments are

$$F_{\mathrm{P}}(\lambda_{\mathrm{ML}},\lambda_{\mathrm{em}}) = c_{\mathrm{instr,P}} I_{\mathrm{ML}}(\lambda_{\mathrm{ML}}) N_{\mathrm{P}}\, A_{\mathrm{eff},k}(\lambda_{\mathrm{ML}}) \Phi_{\mathrm{F,P}} \qquad \text{(A1)}$$

with P = 1: PC; P = 2: PS II; P = 3: PS I; and $c_{\mathrm{instr,\,P}}$ being the calibrating constant of the instrument obtained from the comparison of fluorescence data and spectrochemical determination (Fig. 5); $I_{\mathrm{ML}}(\lambda_{\mathrm{ML}})$ the light intensity of the measuring light of wavelength λ_{ML} (in μE m^{-2} s^{-1}); N_{P} the number of pigment molecules in the sample volume; $\Phi_{\mathrm{F,P}}$ the fluorescence yield of pigment P. $\Phi_{\mathrm{F,PS\ II}}$ and its variability are discussed by Refs. [45–47] and others.

The effective absorption cross section (in m^2) per molecule $A_{\mathrm{eff,P}}(\lambda_{\mathrm{ML}})$ can be more complex due to energy transfer between pigments. $A_{\mathrm{eff,PC}}$ depends only on PC, thus

$$A_{\mathrm{eff,PC}}(\lambda_{\mathrm{ML}}) = A_{\mathrm{PC}}(\lambda_{\mathrm{ML}}) \qquad \text{(A2a)}$$

In the case of the others, always two pigments are involved

$$A_{\mathrm{eff,PS\ II}}(\lambda_{\mathrm{ML}}) = \Phi_{\mathrm{T,PS\ II}}(\lambda_{\mathrm{ML}}) A_{\mathrm{peri,PS\ II}}(\lambda_{\mathrm{ML}}) + A_{\mathrm{core,PS\ II}}(\lambda_{\mathrm{ML}}) \qquad \text{(A2b)}$$

$$A_{\mathrm{eff,PS\ I}}(\lambda_{\mathrm{ML}}) = \Phi_{\mathrm{T,PS\ I}}(\lambda_{\mathrm{ML}}) A_{\mathrm{peri,PS\ I}}(\lambda_{\mathrm{ML}}) + A_{\mathrm{core,PS\ I}}(\lambda_{\mathrm{ML}}) \qquad \text{(A2c)}$$

$\Phi_{\mathrm{P,Q}}$ describes the energy transfer yield from pigment P to pigment Q.

In PBS-containing algae, the peripheral antenna of PS I and PS II is PBS. Thus, the peripheral antenna of PS II and PS I is the same in cyanobacteria and are given as

$$A_{\mathrm{peri,PS\ I}}(\lambda_{\mathrm{ML}}) = A_{\mathrm{peri,PS\ II}}(\lambda_{\mathrm{ML}}) = A_{\mathrm{PC,eff}}(\lambda_{\mathrm{ML}}) = A_{\mathrm{PC}}(\lambda_{\mathrm{ML}}) \qquad \text{(A3)}$$

In PBS-containing algae, the absorption cross section of the peripheral antenna of PS I and PS II is equal to the absorption cross section of the PBS in PE lacking cyanobacteria, and thus proportional to the PC content in the PBS (APC content is neglected). This leads to

$$A_{\mathrm{peri,PS\ II}}(\lambda_{\mathrm{ML}}) = N_{\mathrm{PC}}(\lambda_{\mathrm{ML}})/N_{\mathrm{PS\ II}}\, c_1(\lambda_{\mathrm{ML}}) \quad \text{with } c_1(\lambda_{\mathrm{ML}}) = \text{constant} \qquad \text{(A4a)}$$

and

$$A_{\mathrm{peri,PS\ I}}(\lambda_{\mathrm{ML}}) = N_{\mathrm{PC}}(\lambda_{\mathrm{ML}})/N_{\mathrm{PS\ I}}\, c_2(\lambda_{\mathrm{ML}}) \quad \text{with } c_2(\lambda_{\mathrm{ML}}) = \text{constant} \qquad \text{(A4b)}$$

A.2. Overall fluorescence in PBS-containing algae

The overall fluorescence for a single excitation and emission wavelength is given as a sum of the fluorescence of PC, PS II and PS I:

$$F_{\mathrm{tot}}(\lambda_{\mathrm{ML}},\lambda_{\mathrm{em}}) = F_{\mathrm{PC}}(\lambda_{\mathrm{ML}},\lambda_{\mathrm{em}}) + F_{\mathrm{PS\ II}}(\lambda_{\mathrm{ML}},\lambda_{\mathrm{em}}) + F_{\mathrm{PS\ I}}(\lambda_{\mathrm{ML}},\lambda_{\mathrm{em}}) \qquad \text{(A5)}$$

In the instrument of Fig. 1, there are seven excitation wavelengths (λ_{ML}) and three emission wavelengths (λ_{em}). Thus, Eq. (A6) represents a set of 21 equations. Introducing Eqs. (A1)–(A4b) converts Eq. (A5) to

$$F_{\mathrm{tot}}(\lambda_{\mathrm{ML}},\lambda_{\mathrm{em}}) = [N_{\mathrm{PC}}(k_{1,\lambda\mathrm{ML},\lambda\mathrm{em}} + k_{2,\lambda\mathrm{ML},\lambda\mathrm{em}} + k_{4,\lambda\mathrm{ML},\lambda\mathrm{em}}) + (N_{\mathrm{PS\ II}}\, k_{3,\lambda\mathrm{ML},\lambda\mathrm{em}}) + (N_{\mathrm{PS\ I}}\, k_{5,\lambda\mathrm{ML},\lambda\mathrm{em}})] \qquad \text{(A6)}$$

with the gross rate constants (rate constants because they are fluorescence flux per pigment number)

$$k_{1,\lambda\mathrm{ML},\lambda\mathrm{em}} = I_{\mathrm{ML}}(\lambda_{\mathrm{ML}}) c_{\mathrm{instr,PC}}\, A_{\mathrm{PC}}(\lambda_{\mathrm{ML}}) \Phi_{\mathrm{F,PC}} \qquad \text{(A7a)}$$

$$k_{2,\lambda\mathrm{ML},\lambda\mathrm{em}} = I_{\mathrm{ML}}(\lambda_{\mathrm{ML}}) c_{\mathrm{instr,PS\ II}}\, A_{\mathrm{PC}}(\lambda_{\mathrm{ML}}) c_1(\lambda_{\mathrm{ML}}) \Phi_{\mathrm{T,PS\ II}}(\lambda_{\mathrm{ML}}) \qquad \text{(A7b)}$$

$$k_{3,\lambda\mathrm{ML},\lambda\mathrm{em}} = I_{\mathrm{ML}}(\lambda_{\mathrm{ML}}) c_{\mathrm{instr,PS\ II}}\, A_{\mathrm{core,PS\ II}}(\lambda_{\mathrm{ML}}) \Phi_{\mathrm{F,PS\ II}} \qquad \text{(A7c)}$$

$$k_{4,\lambda ML,\lambda em} = I_{ML}(\lambda_{ML}) c_{instr,PS\ I}\ A_{PC}(\lambda_{ML}) \Phi_{T,PS\ I}(\lambda_{ML}) c_2(\lambda_{ML}) \quad (A7d)$$

$$k_{5,\lambda ML,\lambda em} = I_{ML}(\lambda_{ML}) c_{instr,PS\ I}\ A_{core,PS\ I}(\lambda_{ML}) \Phi_{F,PS\ I} \quad (A7e)$$

In Discussion, it is shown that under most circumstances, these rate constants can be assumed to be constant (independent on species and growth conditions).

The determination of the pigment numbers N_P and of the five gross rate constants from the 14 equations (Eq. (A6)) needs a lot of computer time that may be not available in online applications. As eight unknown parameters need only eight equations, the number of equations is reduced by the following assumptions.

A.2.1. First assumption

The number of PC molecules is proportional to the fluorescence intensity at an excitation wavelength of 610 nm and emission at the 650 nm channel. This means that $c_{instr,PC}\ I_{ML}(\lambda_{ML})\ A_{PC}(\lambda_{ML})\ \Phi_{F,PC}$ is set as constant in Eq. (A1). No interference with PS II and PS I fluorescence is expected.

$$N_{PC} = c_{1,PC} F_{610/650} \quad (A8)$$

Since N_{PC} can be replaced by $F_{610/650}$ in Eq. (A6), only two unknown variables remain in Eq. (A6). Thus, two adequate equations (i.e, $F(\lambda_{1ML,}\ \lambda_{1em})$ and $F(\lambda_{2ML,}\ \lambda_{2em})$) out of the A6 set have to be selected to calculate $N_{PS\ II}$ and $N_{PS\ I}$.

This leads to the following solutions

$$N_{PS\ I} = c_{1,PS\ I} F_{tot}(\lambda_{1ML}, \lambda_{1em}) - c_{2,PS\ I} F_{610/650} - c_{3,PS\ I} F_{tot}(\lambda_{2ML,}\ {}_2\lambda_{em}) \quad (A9a)$$

$$N_{PS\ II} = c_{1,PS\ II} F_{tot}(\lambda_{1ML}, \lambda_{1em}) - c_{2,PS\ II} F_{610/650} - c_{3,PS\ II} F_{tot}(\lambda_{2ML}, \lambda_{2em}) \quad (A9b)$$

The coefficients $c_{1,PC}$, $c_{1,PS\ I}$, $c_{2,PS\ I}$, $c_{3,PS\ I}$ and $c_{1,PS\ II}$, $c_{2,PS\ II}$, $c_{3,PS\ II}$ have to be determined from calibration measurements like those in Fig. 5, where the N_{PC}, $N_{PS\ I}$ and $N_{PS\ II}$ are known from (physico)chemical determinations.

Their relationships with the biophysical gross rate constants are

$$c_{1,PS\ I} = k_{3,\lambda 1ML,\lambda 1em}[(k_{5,\lambda 1ML,\lambda 1em} k_{3,\lambda 2ML,\lambda 2em}) - (k_{5,\lambda 2ML,\lambda 2em} k_{3,\lambda 1ML,\lambda 1em})]^{-1} \quad (A10)$$

$$c_{2,PS\ I} = c_{1,PC}(k_{1,\lambda 1ML,\lambda 1em} + k_{2,\lambda 1ML,\lambda 1em} + k_{4,\lambda 1ML,\lambda 1em}) \times k_{3,\lambda 2ML,\lambda 2em} - (k_{1,\lambda 2ML,\lambda 2em} + k_{2,\lambda 2ML,\lambda 2em} + k_{4,\lambda 2ML,\lambda 2em}) k_{3,\lambda 1ML,\lambda 1em}][(k_{5,\lambda 1ML,\lambda 1em} k_{3,\lambda 2ML,\lambda 2em}) - (k_{5,\lambda 2ML,\lambda 2em} k_{3,\lambda 1ML,\lambda 1em})]^{-1} \quad (A11)$$

$$c_{3,PS\ I} = k_{3,\lambda 2ML,\lambda 2em}[(k_{5,\lambda 1ML,\lambda 1em} k_{3,\lambda 2ML,\lambda 2em}) - (k_{5,\lambda 2ML,\lambda 2em} k_{3,\lambda 1ML,\lambda 1em})]^{-1} \quad (A12)$$

with:

$$c_{1,PS\ II} = k_{5,\lambda 1ML,\lambda 1em}(k_{5,\lambda 2ML,\lambda 2em} k_{3,\lambda 1ML,\lambda 1em} - k_{5,\lambda 1ML,\lambda 1em} k_{3,\lambda 2ML,\lambda 2em})^{-1} \quad (A13)$$

$$c_{2,PS\ II} = c_{1,PC}[k_{5,\lambda 1ML,\lambda 1em}(k_{1,\lambda 2ML,\lambda 2em} + k_{2,\lambda 2ML,\lambda 2em} + k_{4,\lambda 2ML,\lambda 2em}) + (k_{1,\lambda 1ML,\lambda 1em} + k_{2,\lambda 2ML,\lambda 2em} + k_{4,\lambda 2ML,\lambda 2em}) k_{5,\lambda 2ML,\lambda 2em}][(k_{5,\lambda 2ML,\lambda 2em} k_{3,\lambda 1ML,\lambda 1em} - k_{5,\lambda 1ML,\lambda 1em} k_{3,\lambda 2ML,\lambda 2em})]^{-1} \quad (A14)$$

$$c_{3,PS\ II} = (k_{5,\lambda 2ML,\lambda 2em} k_{3,\lambda 1ML,\lambda 1em} - k_{5,\lambda 1ML,\lambda 1em} k_{3,\lambda 2ML,\lambda 2em})^{-1} k_{5,\lambda 2ML,\lambda 2em} \quad (A15)$$

A.2.2. Second assumption

The amount of Chl per PS II and PS I reaction center ($p_{1,Chl}$, and $p_{2,Chl}$, respectively) is supposed to be constant. Under this assumption (whose validity is implied by Fig. 5), the parameters $c_{1,Chl}$ to $c_{3,Chl}$ can be obtained from a fit of the $conc_{Chl}$ (measured by HPLC) to a weighted sum of three fluorescence signals.

$$conc_{Chl} = c_{1,Chl} F_{tot}(\lambda_{1ML}, \lambda_{1em}) + c_{2,Chl} F_{610/650} + c_{3,Chl} F_{tot}(\lambda_{2ML}, \lambda_{2em}) \quad (A16)$$

with the coefficients given by the parameters of Eqs. (A10) and (A15)

$$c_{1,Chl} = (c_{1,PS\ II} + c_{1,PS\ I}),$$
$$c_{2,Chl} = -(c_{2,PS\ II} + c_{2,PS\ I}),$$
$$c_{3,Chl} = -(c_{3,PS\ II} + c_{3,PS\ I}) \quad (A17a - c)$$

During the calibration experiments, Eq. (A17) can be used to control the calibration factors of (Eqs. (A9a), (A9b) and (A16) can be employed to calculate Chl concentration in in situ experiments.

In order to determine cyanobacterial fluorescence in the presence of phytoplankton from other spectral algal groups, it is necessary to deconvolute the measured fluorescence spectra into individual spectra that are assigned to one group

only. This is done by extending the fitting routine of Beutler et al. [15].

Appendix B. Mathematical fit for several excitations wavelengths and detection wavelengths with variable cyanobacterial norm spectra

In order to calculate the fluorescence parameters ($F_{610/650}$, $F_{470/685}$, $F_{610/685}$) for scenario 1 by (Eqs. (A8), (A9b) and (A16), a fit procedure is developed that

- accounts for fluorescence emission from other spectral algal groups in the sample;
- corrects for variations of the cyanobacterial norm spectra;
- evaluates the fit for two emission channels;
- is fast enough for implementation in online analysis.

Therefore, the following matrices and vectors are defined: $\underline{\underline{N_{\lambda em,lem}}}$: (4×7) matrix of algal norm spectra at a single emission wavelength (Fig. 7); $\underline{\underline{C_{\lambda em}}}$: (7×40) matrix of cyanobacterial norm spectra at a single emission wavelength (Fig. 6A,B); $\underline{a_{\lambda em,lem}}$: (1×4) solution vector of phytoplankton concentrations for four phytoplankton groups; $\underline{f_{\lambda em}}$: (1×7) vector, measured F-spectrum at a single detection wavelength (seven excitation wavelengths); λ_{em}: detection wavelength (650 nm; 685 nm in scenario 1).

The variability of the norm spectra of the blue cyanobacteria requires a nonlinear fit routine.

Thus, the fit routine is split into two parts, the core fit and the main fit. The core fit is a subroutine of the main fit. The main fit selects two spectra, one out of the set of 40 norm spectra of the 650-nm detector and one of the 685-nm detector (Fig. 6A,B). These two norm spectra are handed over to the core fit. The core fit uses these individual blue norm spectra and calculates the error sums by linear regression of the two measured spectra at 650 and 685 nm. Under the guidance of a simplex algorithm [70], this procedure is repeated. Finally, the main fit takes that pair of norm spectra and the resulting weighting factors that delivers the minimum error sum as the true fit.

B.1. Core fit

The core fit calculates two linear regressions to approximate the measured spectra at 650 and at 685 nm using the three norm spectra of the three algal groups plus the 650 or 685 nm norm spectrum of the cyanobacteria as proposed by the main fit, if scenario 1 is used. This yields two sets of $a_{\lambda em,lem}$ (concentrations) of the individual groups

$$a_{\lambda em,lem} = \left(N^T_{\lambda em,lem} N_{\lambda em,lem}\right)^{-1} N^T_{\lambda em,lem} f_{\lambda em} \tag{B1}$$

for $\lambda_{em} = 650$ and 685 nm, separately, with the error sum

$$\chi^2_{\lambda em,lem} = \sum_{i=1}^{n_i} \left(f_{i,\lambda em} - \sum_{k=1}^{n_k} a_{k,\lambda em} N_{k,i,\lambda em,lem} \right)^2 \tag{B2}$$

with n_i (number of LEDs) = 7; n_k (number of groups) = 4.

In order to prevent negative elements of the solution vectors, all permutations with one to four algal groups being excluded were tested. The combination of algal groups that has a solution vector without negative elements and yields the smallest error sum is handed over to the main fit.

B.2. Main fit

This algorithm minimizes

$$\chi^2_{l650,l685} = \chi^2_{650,l650} + \chi^2_{685,l685} \tag{B3}$$

by suggesting different pairs of norm spectra with indices $l_{650\ nm} l_{685\ nm}$ to the core fit under the guidance of a simplex algorithm [70]. The first three components of the final solution vector $a_{685,l685}$ provide the concentrations of the three algal groups. The fourth components of $a_{685,l685}$ and $a_{650,l650}$ are taken to calculate the real spectra of the cyanobacteria at 685 and 650 nm. These spectra are used for the analysis described in Appendix A.

References

[1] S. Golubic, S.J. Lee, European Journal of Phycology 34 (1999) 339–348.
[2] A.F. Lotter, Journal of Paleolimnology 25 (2001) 65–79.
[3] J.B. Waterbury, S.W. Watson, R.R.L. Guillard, L.E. Brand, Nature 277 (1979) 293–294.
[4] C.S. Ting, G. Rocap, J. King, S.W. Chisholm, Trends in Microbiology 10 (2002) 134–142.
[5] W.W. Carmichael, Human and Ecological Risk Assessment 7 (2001) 1393–1407.
[6] G.A. Codd, S.G. Bell, K. Kaya, C.J. Ward, K.A. Beattie, J.S. Metcalf, European Journal of Phycology 34 (1999) 405–415.
[7] C.S. Yentsch, C.M. Yentsch, Journal of Marine Research 37 (1979) 471–483.
[8] C.S. Yentsch, D.A. Phinney, Journal of Plankton Research 7 (1985) 617–632.
[9] T.Y. Lee, M. Tsuzuki, T. Takeuchi, K. Yokoyama, I. Karube, Analytica Chimica Acta 302 (1995) 81–87.
[10] T. Lee, M. Tsuzuki, T. Takeuchi, K. Yokoyama, I. Karube, Journal of Applied Phycology 6 (1994) 489–495.
[11] J. Seppala, M. Balode, Hydrobiologia 363 (1998) 207–217.
[12] T.J. Cowles, R.A. Desiderio, S. Neuer, Marine Biology 115 (1993) 217–222.
[13] R.A. Desiderio, C. Moore, C. Lantz, T.J. Cowles, Applied Optics 36 (1997) 1289–1296.
[14] J. Kolbowski, U. Schreiber, in: P. Mathis (Ed.), Photosynthesis: From Light to Biosphere, vol. V, Kluwer Academic Publishing, Dordrecht, 1995, pp. 825–828.
[15] M. Beutler, K.H. Wiltshire, B. Meyer, C. Moldaenke, C. Lüring, M. Meyerhöfer, U.-P. Hansen, H. Dau, Photosynthesis Research 72 (2002) 39–53.

[16] C. Leboulanger, U. Dorigo, S. Jacquet, B. Le Berre, G. Paolini, J. Humbert, Aquatic Microbial Ecology 30 (2002) 23–29.
[17] A.N. Glazer, Journal of Biological Chemistry 264 (1989) 1–4.
[18] D.A. Bryant, The Molecular Biology of Cyanobacteria, Kluwer Academic Publishing, Dordrecht, 1995.
[19] J.J. van Thor, C.W. Mullineaux, H.C.P. Matthijs, K.J. Hellingwerf, Botanica Acta 111 (1998) 430–443.
[20] J. Myers, J.R. Graham, R.T. Wang, Archives of Microbiology 124 (1980) 143–148.
[21] E.M. Gill, B.P. Wittmershaus, Photosynthesis Research 61 (1999) 53–64.
[22] B. Gobets, I.H.M. van Stokkum, M. Rogner, J. Kruip, E. Schlodder, N.V. Karapetyan, J.P. Dekker, R. van Grondelle, Biophysical Journal 81 (2001) 407–424.
[23] C. Müller, W. Reuter, W. Wehrmeyer, H. Dau, H. Senger, Botanica Acta 106 (1993) 480–487.
[24] N.T. Demarsac, J. Houmard, FEMS Microbiology Reviews 104 (1993) 119–189.
[25] W. Reuter, C. Muller, Journal of Photochemistry and Photobiology, B, Biology 21 (1993) 3–27.
[26] M. Kawamura, M. Mimuro, Y. Fujita, Plant and Cell Physiology 20 (1979) 697–705.
[27] H. Schubert, M. Hagemann, FEMS Microbiology Letters 71 (1990) 169–172.
[28] H. Schubert, S. Fulda, M. Hagemann, Journal of Plant Physiology 142 (1993) 291–295.
[29] P.G. Falkowski, J.A. Raven, Aquatic Photosynthesis, Blackwell, Oxford, 1997.
[30] H.C. Riethman, L.A. Sherman, Biochimica et Biophysica Acta 935 (1988) 141–151.
[31] N. Straus, in: D. Bryant (Ed.), The Molecular Biology of Cyanobacteria, Kluwer Academic Publishing, Dordrecht, 1994, pp. 731–750.
[32] E.J. Boekema, A. Hifney, A.E. Yakushevska, M. Piotrowski, W. Keegstra, S. Berry, K.P. Michel, E.K. Pistorius, J. Kruip, Nature 412 (2001) 745–748.
[33] E. Pfundel, Photosynthesis Research 56 (1998) 185–195.
[34] W.P. Williams, J.F. Allen, Photosynthesis Research 13 (1987) 19–45.
[35] J. Biggins, D. Bruce, Photosynthesis Research 20 (1989) 1–34.
[36] D. Campbell, V. Hurry, A.K. Clarke, P. Gustafsson, G. Oquist, Microbiology and Molecular Biology Reviews 62 (1998) 667.
[37] R.R.L. Guillard, C.J. Lorenzen, Journal of Phycology 8 (1972) 10–14.
[38] R. Rippka, M. Herdman, Pasteur culture collection of cyanobacterial strains in axenic culture, Catalogue of Strains, vol. 1, Institut Pasteur, Paris, France, 1992.
[39] O. Van Kooten, J.F.H. Snel, Photosynthesis Research 25 (1990) 147–150.
[40] K.H. Wiltshire, S. Harsdorf, B. Smidt, G. Blocker, R. Reuter, F. Schroeder, Journal of Experimental Marine Biology and Ecology 222 (1998) 113–131.
[41] R.F.C. Mantoura, C.A. Llewellyn, Analytica Chimica Acta 151 (1983) 297–314.
[42] L. Campanella, G. Crescentini, P. Avino, L. Angiello, Annali di Chimica 90 (2000) 153–161.
[43] A. Bennett, L. Bogorad, Journal of Cell Biology 58 (1973) 419–435.
[44] D. Campbell, G. Oquist, Plant Physiology 111 (1996) 1293–1298.
[45] H. Dau, Journal of Photochemistry and Photobiology, B, Biology 26 (1994) 3–27.
[46] H. Dau, Photochemistry and Photobiology 60 (1994) 1–23.
[47] Govindjee, R.S. Knox, J. Amesz, Photosynthesis Research 48 (1996) 1–2.
[48] S. Sandstrom, Y.I. Park, G. Oquist, P. Gustafsson, Photochemistry and Photobiology 74 (2001) 431–437.
[49] Y.I. Park, S. Sandstrom, P. Gustafsson, G. Oquist, Molecular Microbiology 32 (1999) 123–129.
[50] E.G. Andrizhiyevskaya, T.M.E. Schwabe, M. Germano, S. D'Haene, J. Kruip, R. van Grondelle, J.P. Dekker, Biochimica et Biophysica Acta Bioenergetics 1556 (2002) 265–272.
[51] R. MacColl, D. Guard-Friar, Phycobiliproteins, CRC Press, Boca Raton, FL, 1987.
[52] I. Yamazaki, M. Mimuro, T. Murao, T. Yamazaki, K. Yoshihara, Y. Fujita, Photochemistry and Photobiology 39 (1984) 233–240.
[53] M. Mimuro, I. Yamazaki, T. Yamazaki, Y. Fujita, Photochemistry and Photobiology 41 (1985) 597–603.
[54] E. Gantt, Ca. Lipschul, Journal of Phycology 9 (1973) 19–20.
[55] E. Gantt, Ca. Lipschul, Biochimica et Biophysica Acta 292 (1973) 858–861.
[56] G.F.W. Searle, J. Barber, G. Porter, C.J. Tredwell, Biochimica et Biophysica Acta 501 (1978) 246–256.
[57] A.R. Holzwarth, J. Wendler, W. Wehrmeyer, Photochemistry and Photobiology 36 (1982) 479–487.
[58] T. Gillbro, A. Sandstrom, V. Sundstrom, A.R. Holzwarth, FEBS Letters 162 (1983) 64–68.
[59] J. Wendler, A.R. Holzwarth, W. Wehrmeyer, Biochimica et Biophysica Acta 765 (1984) 58–67.
[60] T. Gillbro, A. Sandstrom, V. Sundstrom, J. Wendler, A.R. Holzwarth, Biochimica et Biophysica Acta 808 (1985) 52–65.
[61] G.W. Suter, A.R. Holzwarth, Biophysical Journal 52 (1987) 673–683.
[62] R. Vangrondelle, J.P. Dekker, T. Gillbro, V. Sundstrom, Biochimica et Biophysica Acta Bioenergetics 1187 (1994) 1–65.
[63] K. Csatorday, R. Maccoll, V. Csizmadia, J. Grabowski, C. Bagyinka, Biochemistry 23 (1984) 6466–6470.
[64] K. Sauer, H. Scheer, Biochimica et Biophysica Acta 936 (1988) 157–170.
[65] A.R. Holzwarth, E. Bittersmann, W. Reuter, W. Wehrmeyer, Biophysical Journal 57 (1990) 133–145.
[66] G. Harnischfeger, G.A. Codd, Biochimica et Biophysica Acta 502 (1978) 507–513.
[67] M. Mimuro, Y. Fujita, Biochimica et Biophysica Acta 504 (1978) 406–412.
[68] T. Redlinger, E. Gantt, Proceedings of the National Academy of Sciences of the United States of America-Biological Sciences 79 (1982) 5542–5546.
[69] A.C. Ley, Plant Physiology 74 (1984) 451–454.
[70] J.A. Nelder, R. Mead, Computer Journal 7 (1965) 308–313.